Identification of the stereochemical requirements in the 4-aryl-2-cycloalkylidenhydrazinylthiazole scaffold for the design of selective human monoamine oxidase B inhibitors

ARTICLE *in* BIOORGANIC & MEDICINAL CHEMISTRY · APRIL 2014

Impact Factor: 2.79 · DOI: 10.1016/j.bmc.2014.03.042 · Source: PubMed

Bioorganic & Medicinal Chemistry 22 (2014) 2887–2895

Contents lists available at ScienceDirect

Bioorganic & Medicinal Chemistry

journal homepage: www.elsevier.com/locate/bmc

Identification of the stereochemical requirements in the 4-aryl-2-cycloalkylidenhydrazinylthiazole scaffold for the design of selective human monoamine oxidase B inhibitors

Melissa D'Ascenzio [a], Simone Carradori [a,*], Daniela Secci [a], Luisa Mannina [a,e], Anatoly P. Sobolev [e], Celeste De Monte [a], Roberto Cirilli [b], Matilde Yáñez [c], Stefano Alcaro [d], Francesco Ortuso [d]

[a] Dipartimento di Chimica e Tecnologie del Farmaco, Sapienza University of Rome, P.le A. Moro 5, 00185 Rome, Italy
[b] Istituto Superiore di Sanità, Dipartimento del Farmaco, V.le Regina Elena 299, 00161 Rome, Italy
[c] Departamento de Farmacología, Facultad de Farmacia, Universidad de Santiago de Compostela, Campus Universitario Sur, E-15782 Santiago de Compostela (La Coruña), Spain
[d] Dipartimento di Scienze della Salute, 'Magna Graecia' University of Catanzaro, Campus Universitario 'S. Venuta', Viale Europa Loc. Germaneto, 88100 Catanzaro, Italy
[e] Istituto di Metodologie Chimiche, Laboratorio di Risonanza Magnetica 'Annalaura Segre', CNR, via Salaria km 29.300, 00015 Monterotondo, Rome, Italy

ARTICLE INFO

Article history:
Received 12 January 2014
Revised 21 March 2014
Accepted 27 March 2014
Available online 5 April 2014

Keywords:
Monoamine oxidase inhibitors
Methylcyclopentane
Diastereoseparation
Molecular modeling
Thiazole

ABSTRACT

Exploring the effect that substituents on the cycloaliphatic ring had on the inhibitory activity against human monoamine oxidase B of a series of 4-aryl-2-cycloalkylidenhydrazinylthiazoles led to the synthesis of a new series of 2-methylcyclopentyl and 3-methylcyclopentyl derivatives which were tested in vitro as mixtures of diastereoisomers. In fact, due to the presence of a chiral center on the cycloaliphatic ring and a trisubstituted C=N bond, they exist as four diastereoisomers ((*E*)-(*R*), (*E*)-(*S*), (*Z*)-(*R*), (*Z*)-(*S*)). 4-(2,4-Difluorophenyl)-2-(2-(3-methylcyclopentylidene)hydrazinyl)thiazole was chosen as a model to investigate the influence of stereochemical requirements on the inhibitory activity against hMAO-B of these derivatives after a stereoconservative synthesis and semi-preparative HPLC diastereoseparation. (*R*)-(*Z*) isomer of this compound was endowed with a potent and selective hMAO-B inhibition higher than that of reference drugs as also corroborated by molecular modeling studies.

1. Introduction

Human monoamine oxidases (hMAOs) are FAD-dependent enzymes which are involved in the oxidative deamination of endogenous and exogenous primary, secondary and tertiary amines. Located on the outer mitochondrial membrane, hMAOs play a fundamental physiological role in the regulation of monoaminergic neurotransmissions by controlling the amounts of dopamine (DA), adrenaline (A) and noradrenaline (NA) inside the synaptic cleft. In the brain, hMAOs are present in two isoforms, hMAO-A and hMAO-B, which differ in distribution, substrate specificity, and sensibility to inhibitors. Inhibition of hMAOs, in fact, represents the rationale for the treatment of those pathologies in which there is an impairment of synaptic transmission, such as depressive disorders and neurodegenerative diseases.[1] However, one of the main limitations to the use of non-selective MAO-inhibitors is the high prevalence of hMAO-A in the gastrointestinal tract, where it is mainly involved in the metabolism of an exogenous monoamine: *p*-tyramine. Although *p*-tyramine cannot cross the blood brain barrier, it can behave as a peripheral adrenergic agonist and cause dangerous hypertensive crisis: the so called cheese-effect. The safety of hMAO-inhibitors has been considerably increased by the introduction of selective anti-hMAO-B agents, which are endowed with high therapeutic potential against neurodegenerative disorders like Parkinson's and Alzheimer's disease, but devoid of unwanted peripheral effects.[2] In fact, hMAO-B is highly expressed in astrocytes around senile plaques and its activity is notably increased in patients with age-related gliosis and Alzheimer's disease. hMAO-B selective inhibition is expected to enhance dopaminergic neurotransmission, which is beneficial for PD, and to reduce the oxidative stress exerted on neurons by hydrogen peroxide, a byproduct of MAO-catalyzed deamination of neurotransmitters, resulting in a neuroprotective and neurorestorative effects.[3,4] Therefore, there is a considerable interest in obtaining potent and selective MAO inhibitors.[5]

For several years our group has been working on hMAO-B inhibitors as potential co-adjuvants for the treatment of neurodegenerative diseases:[6] we recently reported on the promising in vitro activity and selectivity of a large number of 4-aryl-2-hydrazinylthiazoles.[7–15]

* Corresponding author. Tel.: +39 06 49913149; fax: +39 06 49913923.
E-mail address: simone.carradori@uniroma1.it (S. Carradori).

http://dx.doi.org/10.1016/j.bmc.2014.03.042
0968-0896/

3D-QSAR studies helped to rationalize experimental results and to provide robust structure-activity relationships: (i) the aryl group at C4 of the thiazole is responsible for the correct orientation of the inhibitor inside the active site of hMAO-B and directly interacts with two tyrosine residues (the so called 'aromatic cage') close to the catalytic FAD;[10] (ii) in order to obtain productive interactions within the aromatic cage, the aryl moiety has to be *ortho* and/or *para* substituted with an electron-withdrawing group (NO_2, CN, F), (iii) the introduction of substituents on the C5 of the thiazole and/or highly hindered substituents on the C4 (naphthalene, coumarin) determines a dramatic loss of activity and selectivity;[12] (iv) 5- or 6-membered cycloaliphatic and small heteroaromatic rings (furan, thiophene and pyridine) are preferred on the *N*1 of the hydrazine.[8,13,14]

Moreover, we discovered that (*R*)-enantiomers of some reported chiral derivatives (2-methyl- and 3-methylcyclohexylidene derivatives) were generally responsible for the higher activity and selectivity of racemates against hMAO-B.[8–13] Following this rationale, we designed a new series of 4-aryl-2-cyclopentylidenhydrazinylthiazole derivatives in which a methyl group was introduced on the C2 or the C3 of the cycloaliphatic nucleus. The effects that this chemical modification had on activity and selectivity of the obtained derivatives were evaluated by determining the IC_{50} of tested compounds against both hMAO-A and hMAO-B. Biological results showed that these compounds were all able to inhibit hMAO-B at nanomolar concentrations when tested as mixtures of diastereoisomers. In order to further investigate the stereochemical requirements for optimal hMAO-B inhibition, one of the synthesized derivatives was chosen as a model: (*E*)-(*R*) and (*Z*)-(*R*) diastereoisomers of 4-(2,4-difluorophenyl)-2-(2-(3-methylcyclopentylidene)hydrazinyl)thiazole were synthesized via a stereoconservative route, separated by chiral semi-preparative HPLC on polysaccharide-based stationary phase, and individually tested against hMAO-A and hMAO-B.

2. Chemistry

Compounds **1**–**8** were synthesized in high yields (81–99%) as mixtures of diastereoisomers according to an improved MW-assisted protocol developed in our laboratory (Scheme 1).

2-Methyl-/3-methylcyclopentanone was reacted with thiosemicarbazide under MW irradiation (103 °C, 5 min, 300 W) in the presence of catalytic amounts of acetic acid. The obtained thiosemicarbazones were subsequently converted into the corresponding 4-aryl-2-hydrazinylthiazole derivatives by reaction with the corresponding α-halo-2-/2,4-substituted-acetophenones in methanol under MW irradiation (90 °C, 10 min, 300 W). All synthesized products were washed with petroleum and diethyl ether, purified by column chromatography (ethyl acetate/*n*-hexane; 1:1), and characterized by spectroscopic methods and elemental analysis.

The use of commercially available (*R*)-3-methylcyclopentanone as starting material allowed synthesizing compound **8** as a single enantiomer ((*R*)-**8**) via a stereoconservative pathway (Scheme 2).

Accurate analyses of ^{1}H NMR spectra ($CDCl_3$, 400 MHz) revealed that the obtained compounds were a mixture of *E* and *Z* geometric isomers, the *ratio* of which could be measured by integrating the area of the corresponding N*H* signal (see ^{1}H NMR characterization data), whereas CH_3 signals were often overlapped and did not allow an accurate discrimination between the two isomers. According to previous theoretical and chromatographic study for similar compounds, the choice of a polar protic solvent as reaction medium (methanol) should favor the *E*-configuration and limit the interconversion between the two isomers.[16–18]

3. HPLC diastereoseparation

The first step of our chromatographic experiments was carried out with the aim to find a chiral HPLC system capable of simultaneously separating the four stereoisomers of rac-**8**: ((*E*)-(*R*), (*Z*)-(*R*), (*E*)-(*S*), and (*Z*)-(*S*). As shown in Figure 1a, a clear resolution of all the peaks was not possible in any of the conditions screened. However, diasteroseparation of *E* and *Z* stereoisomers was possible when enantiopure (*R*)-**8** was injected in a column charged with Chiralpak AD CSP under normal phase conditions (Figure 1b). The absolute configuration of the thiazole derivatives in homochiral form was assigned by chemical correlation.

The two peaks of (*R*)-**8** were characterized by the same specific rotation sign and similar area. It was found that the diastereomeric ratio (*Z*/*E*), measured at the isosbestic point of 254 nm, was 46/54 similar to that obtained by ^{1}H NMR spectroscopy (43/57). This value indicated that the stability of the second eluting diastereomer ((*E*)-(*R*)-**8**) was only slightly higher than the first eluting one ((*Z*)-(*R*)-**8**).

The same HPLC separation conditions were used on a semi-preparative scale to isolate mg-amounts of each (*R*)-**8** isomer with high degree of diastereomeric purity (Fig. 1c and d). In this way, tens of a milligram of pure stereoisomers (*E*)-(*R*)-**8** and (*Z*)-(*R*)-**8** were made available for separate biological evaluation (Scheme 3).

4. NMR assignment of eluted stereoisomers

In order to clarify the stereochemistry of the products eluted [(*Z*)-(*R*)-**8** and (*E*)-(*R*)-**8**] from the chromatographic separation regarding the C=N double bond, an NMR study was performed using 1D and 2D NMR (^{1}H–^{1}H COSY and ^{1}H–^{1}H NOESY) techniques. More in detail, the ^{1}H–^{1}H NOESY experiment allows the detection of spatial proximities between ^{1}H spins by taking advantage of the dipolar coupling interaction. It can bring valuable information such as double-bond configuration and spatial organization which would be otherwise very difficult—if not impossible—to obtain.

The ^{1}H–^{1}H NOESY map of the first eluted product (data not shown), shows a NOE contact between NH at 10.58 ppm and CH_2-a protons at 1.88 and 2.66 ppm indicating their spatial proximity and therefore suggesting a (*Z*)-configuration. In the case of the second eluted product, NOE contacts between NH at

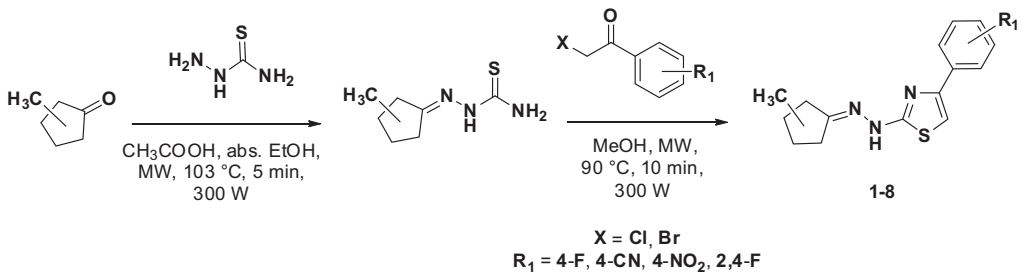

Scheme 1. General synthetic pattern of synthesized derivatives.

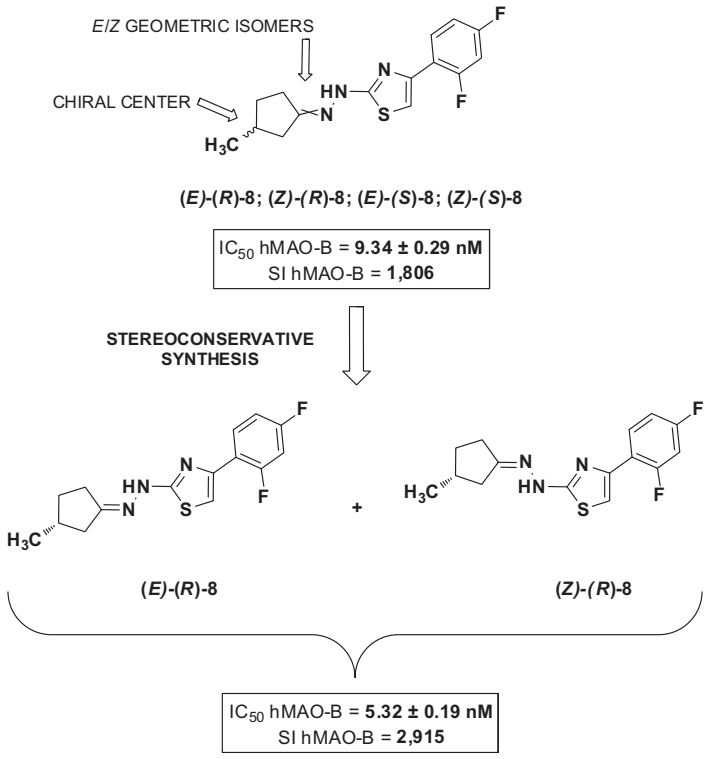

Scheme 2. Stereoconservative synthesis of *E* and *Z* isomers of compound (*R*)-**8**.

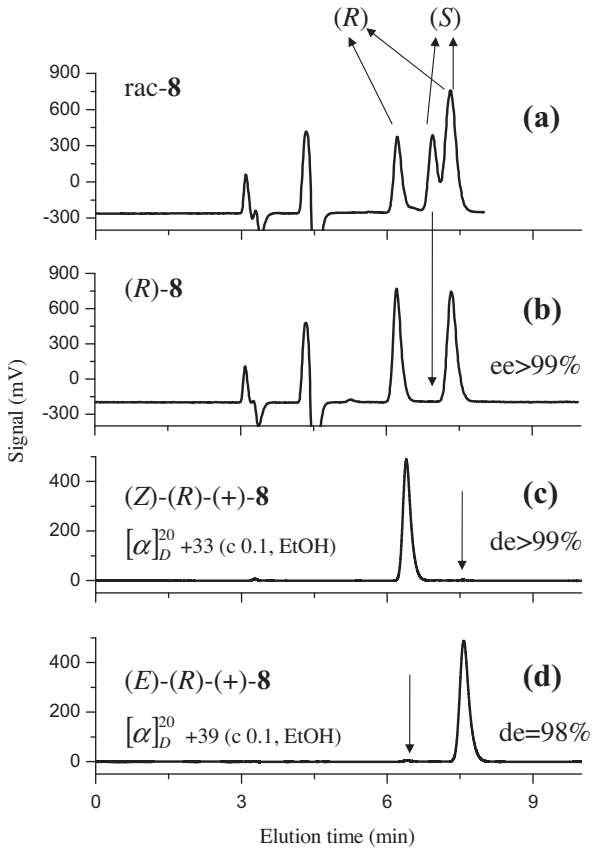

Figure 1. HPLC traces of rac-**8** (a) and (*R*)-**8** (b), and semi-preparative isolation of *Z* and *E* isomers of (*R*)-**8** (c and d). Column: Chiralpak AD (250 mm × 4.6 mm I.D.); mobile phase: *n*-hexane/2-propanol 90:10 (v/v); flow rate: 1 mL/min; detector: UV at 254 nm; temperature: 25 °C.

10.60 ppm and CH_2-d protons at 2.30 and 2.50 ppm were observed implying the (*E*)-configuration of C=N double bond (Scheme 3).

5. Pharmacology

Compounds **1**–**8** were evaluated for their ability to inhibit hMAOs as mixtures of diastereomers, while the *E* and *Z* isomers of (*R*)-**8** were tested both individually and as a mixture. The biological activity of tested compounds was investigated using the Amplex® Red MAO assay kit and microsomal MAO isoforms prepared from insect cells (BTI-TN-5B1-4) infected with recombinant baculovirus containing cDNA inserts for hMAO-A or hMAO-B.[19] *p*-Tyramine was chosen as common substrate for both hMAO-A and hMAO-B. The reduction of the amount of hydrogen peroxide (H_2O_2) produced by hMAOs catabolic activity was measured using 10-acetyl-3,7-dihydroxyphenoxazine (Amplex® Red reagent), a non-fluorescent and highly sensitive probe that reacts with H_2O_2 in the presence of horseradish peroxidase to produce the fluorescent product resorufin. Both tested compounds and reference inhibitors were unable to directly react with Amplex® Red reagent, indicating that these drugs were not interfering with the measurements.

Under our experimental conditions, hMAO-A displayed a Michaelis constant (K_m) equal to 457.17 ± 38.62 μM and a maximum reaction velocity (V_{max}) in the control group of 185.67 ± 12.06 nanomol *p*-tyramine/min/mg protein, whereas hMAO-B showed a K_m of 220.33 ± 32.80 μM and a V_{max} equal to 24.32 ± 1.97 nanomol *p*-tyramine/min/mg protein ($n = 5$). Most tested drugs concentration-dependently inhibited this enzymatic control activity (Table 1).

6. Results and discussion

Inhibition data, including selectivity index (ratio), against hMAO-A and -B are presented in Table 1. All compounds bearing

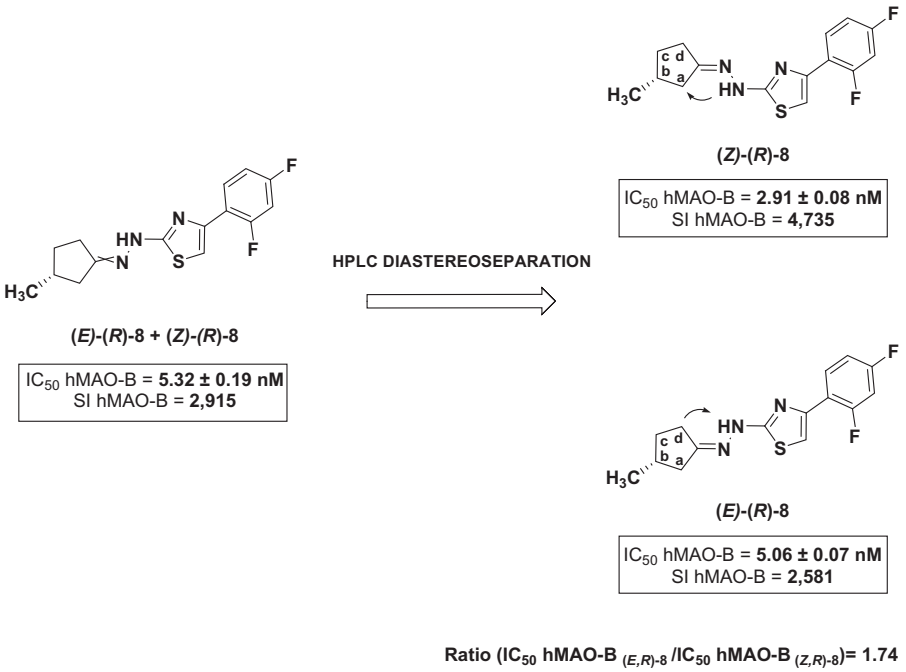

Scheme 3. Chemical approach to the determination of the relationship between structure and activity in the 4-aryl-2-hydrazinylthiazole scaffold.

Table 1
Structure and biological activity of new derivatives and reference compounds after a 15 min preincubation period with human MAO isoforms

Compound	R	R_1	IC_{50} hMAO-A	IC_{50} hMAO-B	Ratio
1	2-CH_3	4-F	4.58 ± 0.32 μM[a]	9.13 ± 0.32 nM	502
2	2-CH_3	4-NO_2	19.23 ± 0.96 μM[a]	8.31 ± 0.21 nM	2314
3	2-CH_3	4-CN	4.31 ± 0.21 μM[a]	38.03 ± 0.96 nM	113
4	2-CH_3	2,4-F	10.93 ± 0.67 μM[a]	6.16 ± 0.15 nM	1774
5	3-CH_3	4-F	1.89 ± 0.01 μM[a]	65.49 ± 4.35 nM	30
6	3-CH_3	4-NO_2	[**]	375.71 ± 12.45 nM	>266[b]
7	3-CH_3	4-CN	11.09 ± 0.59 μM[a]	227.48 ± 11.85 nM	49
8	3-CH_3	2,4-F	16.87 ± 0.64 μM[a]	9.34 ± 0.29 nM	1806
(*R*)-**8**	3-CH_3	2,4-F	15.51 ± 0.75 μM[a]	5.32 ± 0.19 nM	2915
(*Z*)-(*R*)-**8**	3-CH_3	2,4-F	13.78 ± 0.05 μM[a]	2.91 ± 0.08 nM	4735
(*E*)-(*R*)-**8**	3-CH_3	2,4-F	13.06 ± 0.08 μM[a]	5.06 ± 0.07 nM	2581
Clorgyline			4.46 ± 0.32 nM[a]	61.35 ± 1.13 μM	0.000073
(*R*)-(−)-Deprenyl			67.25 ± 1.02 μM[a]	19.60 ± 0.86 nM	3431
Iproniazid			6.56 ± 0.76 μM	7.54 ± 0.36 μM	0.87
Moclobemide			361.38 ± 19.37 μM	[*]	<0.36[c]
Isatin			[**]	18.75 ± 1.24 μM	>5.3[b]

Ratio: hMAO-B selectivity index = $IC_{50(hMAO-A)}/IC_{50(hMAO-B)}$. Each IC_{50} value is the mean ± S.E.M. from five experiments ($n = 5$).
[a] Level of statistical significance: $P < 0.01$ versus the corresponding IC_{50} values obtained against hMAO-B, as determined by ANOVA/Dunnett's.
[*] Inactive at 1 mM (highest concentration tested).
[**] Inactive at 100 μM (highest concentration tested). At higher concentrations the compounds precipitate.
[b] Value obtained under the assumption that the corresponding IC_{50} against hMAO-A is the highest concentration tested (100 μM).
[c] Value obtained under the assumption that the corresponding IC_{50} against hMAO-B is the highest concentration tested (1 mM).

2-/3-methylcyclopentylidene substituent at N1-hydrazine inhibit hMAO-B in the nanomolar range, as expected on the basis of our previous works on structurally similar derivatives (2- and 3-methylcyclohexylidene derivatives).[8–13]

In general, 2-methylcyclopentylidene derivatives (**1**–**4**) were better inhibitors towards human MAO-B (see compound **2**, IC_{50} = 8.31 ± 0.21 nM and ratio >2314) than the corresponding 3-methylcyclopentylidene counterparts (**5**–**8**). The inhibitory activity and selectivity towards the B isoform is favored by *ortho*/*para* disubstitution of the phenyl ring with electron-withdrawing groups (especially with the presence of fluorine atoms), thus confirming the fundamental role that the dipolar moment of the inhibitor plays in the interaction with the aromatic cage in the active site of the enzyme. Although 3-methylcyclopentylidene derivatives (**5**–**8**) showed a slightly lower inhibitory activity against hMAO-B (see compound **8**, IC_{50} = 9.34 ± 0.29 nM and ratio >1806) their IC_{50} were, however, comparable to the reference drug (*R*)-(−)-deprenyl 19.60 ± 0.86 nM), with the only exception of compounds **6** and **7**. As in the previously studied 2- and 3-methylcyclohexylidene analogues, where the stereochemistry of the methyl substituent on the cycloaliphatic ring was an important modulator of biological activity, we were prompted to study this phenomenon with regards to the newly synthesized 2- and 3-methylcyclopentylidene derivatives. For this purpose, compound **8** was synthesized as single enantiomer starting from commercially available (*R*)-3-methylcyclopentanone, and its *E* and *Z* stereoisomers were tested both as a mixture and as single isomers after HPLC semi-preparative resolution. As expected, the enantiopure *E* and *Z* isomers

Table 2
Docking descriptors of (*Z*)-(*R*)-**8** and (*E*)-(*R*)-**8** hMAOs recognition. GScoreXP and ΔE_{int} data are reported in kcal/mol

Compound	hMAO-A		hMAO-B	
	GScoreXP	ΔE_{int}	GScoreXP	ΔE_{int}
(*Z*)-(*R*)-**8**	−0.643	−18.47	−10.004	−49.66
(*E*)-(*R*)-**8**	−2.012	−19.03	−9.620	−48.82

showed higher activity and selectivity against hMAO-B than the racemic one (Scheme 2) and the (*Z*)-(*R*)-**8** isomer, in particular, displayed a surprising inhibitory activity (IC_{50} hMAO-B = 2.91 ± 0.08 nM) and an excellent hMAO-B selectivity (ratio = 4735), which was higher than that of the most potent reference drug and about two-fold than that of the parent compound ((*R*)-**8**). As a matter of this, a molecular modeling approach confirmed the essential stereochemical requirements for this heterocyclic scaffold to obtain potent and selective hMAO-B inhibitors.

The hMAO-A and -B recognition of both *E* and *Z* isomers of (*R*)-**8** was evaluated by means of docking techniques. According to experimental IC_{50} data, docking scoring function (GScoreXP) and theoretical interaction energy (ΔE_{int}) strongly remarked the better accommodation of both *E* and *Z* isomers of (*R*)-**8** into the hMAO-B active site with respect to the hMAO-A one (Table 2).

The docking poses analysis addressed the previously reported isozyme preference to the known broader binding site of hMAO-B with respect to hMAO-A. A *per residue* binding energy evaluation revealed a larger number of amino acids involved in the hMAO-B recognition of both (*R*)-**8** isomers. Moreover, while in hMAO-B all interacting residues reported productive interaction energy to our inhibitors, in hMAO-A four residues, Lys305, Phe352, Tyr407 and Tyr444 showed disfavoring contribution, due to steric clashes, to the ligands recognition (Fig. 2).

The configuration of the double bond did not remarkably influence the binding modes of (*R*)-**8**, actually *E* and *Z* isomers showed quite similar recognition in both hMAOs. In all cases, the difluorophenyl ring was oriented toward the FAD cofactor and the chiral 3-methylcyclopentyl was located at the binding cleft entrance site. In the hMAO-B, the methylcyclopentyl moiety found a better accommodation into a lipophilic cage whereas in hMAO-A such an area is hidden by Phe208. The substitution of hMAO-A Ile180, Asn181, Phe208 and Ile335 with the corresponding hMAO-B Leu171, Cys172, Ile199 and Tyr326 respectively, strongly modify the shape of the active site and, as a consequence, the orientation of the thiazole ring (Fig. 3). The different shape and the hMAO-A active site volume smaller than hMAO-B, could also explain the previously reported bumps among our inhibitors and some residues of former isozyme.

7. Conclusion

We designed and synthesized new 4-aryl-2-cycloalkylidenhydrazinylthiazoles with the aim of investigating the stereochemical requirements in this scaffold regarding the hMAO inhibition. According to what we demonstrated with 2- and 3-methylcyclohexylidene derivatives, these 2- and 3-methylcyclopentylidene compounds displayed good inhibitory activity and high selectivity against hMAO-B. Moreover, (*R*)-**8** stereoisomer, obtained by a stereoconservative synthesis, was a two-fold selective hMAO-B inhibitor than the racemic mixture. With respect to *E*/*Z* isomers, we performed a semi-preparative HPLC to separate and test each geometric isomer of this potent derivative. Biological assays stated the best and more selective hMAO-B inhibition (two-fold) by (*Z*)-(*R*)-(**8**) proposing a stereospecific enzyme recognition of the inhibitor. These results were also corroborated by computational studies. Molecular modeling addressed to steric hindrance the different affinity of both *E* and *Z* isomers of (*R*)-**8** with respect to hMAO-A and -B. Actually, the recognition was driven by the known larger volume of the hMAO-B active site with respect to the hMAO-A one.

8. Experimental section

8.1. Chemistry

Starting materials and reagents were obtained from commercial suppliers and were used without further purification. Microwave-assisted reactions were performed in a Biotage Initiator™ 2.0 (Uppsala, Sweden). Melting points (mp) were determined by the capillary method on an FP62 apparatus (Mettler-Toledo) and are uncorrected. ^{1}H and ^{13}C NMR spectra were recorded at 400 or 600 MHz on a Bruker spectrometer using DMSO-d_6 or $CDCl_3$ as solvents. Chemical shifts are expressed as δ units (ppm) relative to TMS. Coupling constants *J* are expressed in hertz (Hz). IR spectra were registered on a Perkin–Elmer FTIR Spectrometer Spectrum 1000 in anhydrous potassium bromide. Elemental analyses for C, H, and N were determined with a Perkin–Elmer 240 B microanalyzer and the analytical results were within ±0.4% for all compounds. All reactions were monitored by TLC on 0.2 mm thick silica gel plates (60 F_{254} Merck). Preparative flash column chromatography was carried out on silica gel (230–400 mesh, G60 Merck). Organic solutions were dried over anhydrous sodium sulfate. Concentration and evaporation of the solvent after reaction or extraction

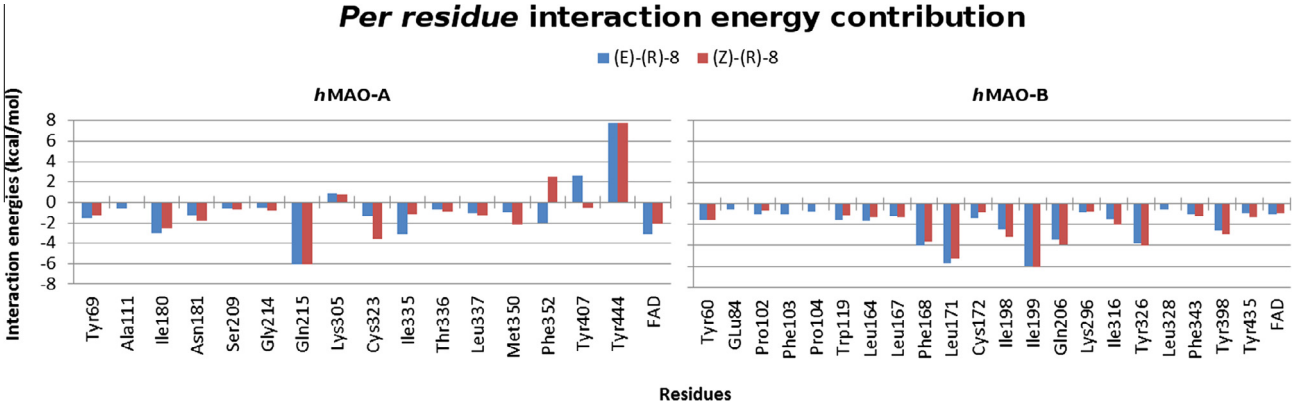

Figure 2. hMAO-A and -B *per residue* interaction energy contribution to (*E*)-(*R*)-**8** and (*Z*)-(*R*)-**8** recognition.

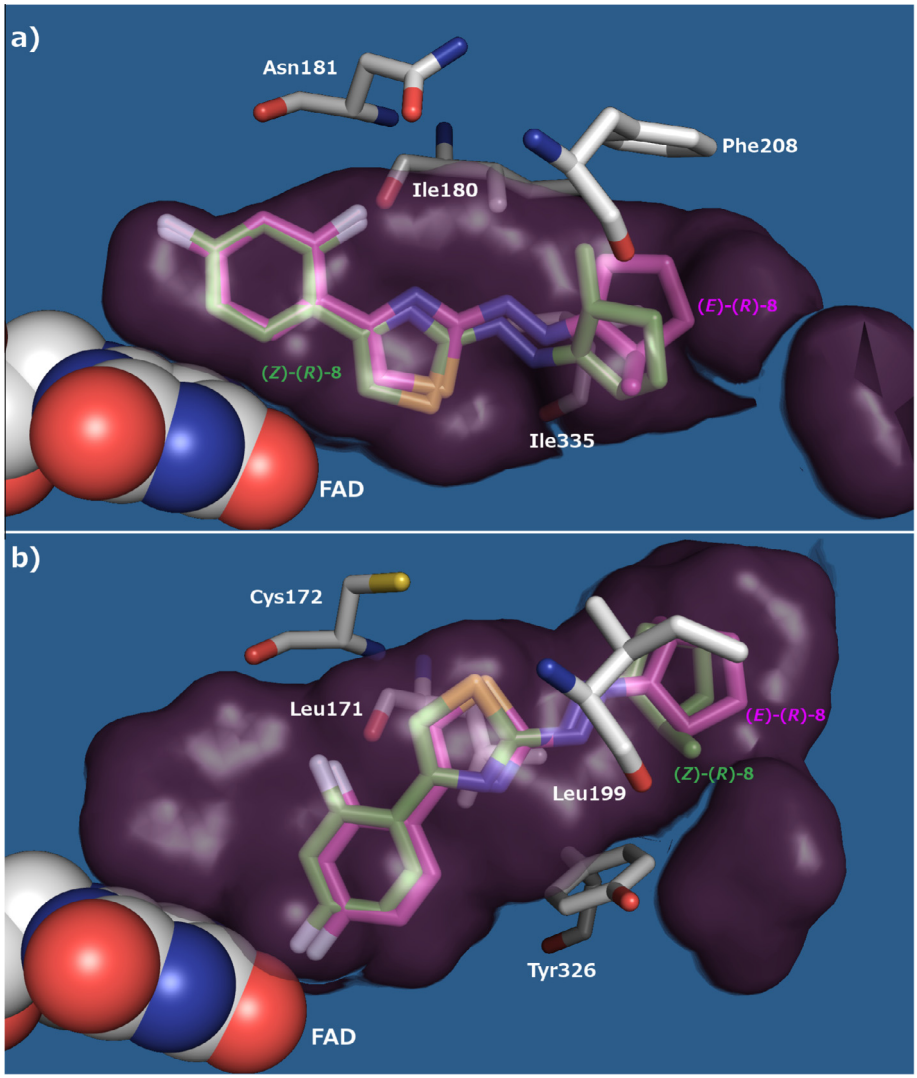

Figure 3. Docking best poses of both *E* and *Z* isomers of (*R*)-**8** into the (a) hMAO-A and (b) hMAO-B. Binding site shapes are depicted in transparent plum surface, the inhibitor *E* and *Z* isomers are in polytube purple or green carbon atoms respectively, hMAO-A and -B mutated residues are in polytube white carbon atoms, FAD cofactor is reported in spacefill CPK colored.

were carried out on a rotary evaporator (Büchi Rotavapor) operating at reduced pressure.

8.2. General procedure for the MW-assisted synthesis of thiosemicarbazone intermediates

In a 5 mL vessel suitable for microwave reactor (2.45 GHz high-frequency microwaves, power range 0–300 W) 2- or 3-methylcyclopentanone (3.4 mmol) and acetic acid (2–3 drops) were added to a suspension of thiosemicarbazide (0.30 g, 3.4 mmol) in 2 mL of absolute ethanol. After the vessel was securely sealed, the mixture was pre-stirred for 30 s and then heated up to 103 °C by microwave irradiation for 5 min. If not set, the irradiation power reaches its maximum at the beginning of reaction and then it decreases to lower and constant values. The vial internal temperature was controlled by an equipped IR sensor. After cooling the reaction down to room temperature using a stream of pressurized air, the obtained suspension was filtered and the solid washed with petroleum ether, *n*-hexane, and diethyl ether. The crude mixture was purified by column chromatography (SiO_2, ethyl acetate/*n*-hexane) to give the desired thiosemicarbazone derivatives.

8.3. General procedure for the MW-assisted synthesis of derivatives (1–8 and (*R*)-8)

The thiosemicarbazone intermediates (1.5 mmol) were added to a solution of the correspondent α-halo-2-/2,4-substituted-acetophenone in 2 mL of methanol. The mixture was pre-stirred in a sealed vessel for 1 min and then heated up to 90 °C by microwave irradiation for 10 min. The reaction was cooled down with pressurized air, filtered, and the obtained solid washed with *n*-hexane and diethyl ether. The crude mixture was purified by column chromatography (SiO_2, ethyl acetate/*n*-hexane 1:1) to give desired compounds in high yields (81–99%).

8.4. Characterization data for new compounds (obtained as a mixture of *E*/*Z* isomers)

8.4.1. 1-(4-(4-Fluorophenyl)thiazol-2-yl)-2-(2-methylcyclopentylidene)hydrazine (1)

E/*Z* ratio: 56/44. Yield 98%; mp 174–176 °C; IR cm^{-1} (KBr): 1612 (C=N), 1229 (Ar-F); ^1H NMR ($CDCl_3$, 600 MHz) δ 1.20–1.22 (d, J = 6.8 Hz, 3H, CH_3), 1.35–1.36 (m, 1H, cyclopentyl), 1.54–1.55 (m,

1H, cyclopentyl), 1.77–1.78 (m, 1H, cyclopentyl), 2.01–2.03 (m, 1H, cyclopentyl), 2.12–2.14 (m, 1H, cyclopentyl), 2.55–2.57 (m, 1H, cyclopentyl), 2.74–2.76 (m, 1H, cyclopentyl), 6.63 (s, 1H, C_5H-thiazole), 7.18–7.20 (dd, J_{HH} = 8.6 Hz, J_{HF} = 8.6 Hz, 2H, Ar), 7.70–7.72 (dd, J_{HH} = 8.6 Hz, J_{HF} = 5.0 Hz, 2H, Ar), 12.35 (br s, 1H, (*E*)-N*H*, D_2O exch.), 14.25 (br s, 1H, (*Z*)-N*H*, D_2O exch.). ^{13}C NMR ($CDCl_3$, 150 MHz) δ 16.70 (CH_3), 22.71 (CH_2, cyclopentyl), 30.50 (CH, cyclopentyl), 33.95 (CH_2, cyclopentyl), 40.15 (CH_2, cyclopentyl), 100.21 (CH, thiazole), 116.93 (d, J_{C-F} = 22 Hz, CH, Ar), 123.99 (d, J_{C-F} = 3.5 Hz, C, Ar), 127.82 (d, J_{C-F} = 6.7 Hz, CH, Ar), 139.54 (C, thiazole), 163.80 (d, J_{C-F} = 252 Hz, CF, Ar), 169.65 (C, thiazole), 174.85 (C=N). Anal. Calcd for $C_{15}H_{16}FN_3S$: C, 62.26; H, 5.57; N, 14.52. Found: C, 62.57; H, 5.39; N, 14.39.

8.4.2. 1-(2-Methylcyclopentylidene)-2-(4-(4-nitrophenyl)thiazol-2-yl)hydrazine (2)

Yield 97%; mp 170–172 °C; cm^{-1} (KBr): 1629 (C=N), 1510 and 1339 (NO_2); ^1H NMR (DMSO-d_6, 400 MHz) δ 1.09 (br s, 3H, CH_3), 1.28–1.29 (m, 1H, cyclopentyl), 1.64–1.65 (m, 1H, cyclopentyl), 1.87–1.88 (m, 1H, cyclopentyl), 1.97–1.98 (m, 1H, cyclopentyl), 2.23–2.25 (m, 1H, cyclopentyl), 2.58–2.60 (m, 1H, cyclopentyl), 2.61–2.63 (m, 1H, C_2H), 7.63 (s, 1H, C_5H-thiazole), 8.09–8.11 (d, J = 7.8 Hz, 2H, Ar), 8.26–8.28 (d, J = 7.8 Hz, 2H, Ar), 10.75 (br s, 1H, N*H*, D_2O exch.); ^{13}C NMR (DMSO-d_6, 101 MHz) δ 17.33 (CH_3), 22.72 (CH_2, cyclopentyl), 29.28 (CH, cyclopentyl), 33.88 (CH_2, cyclopentyl), 108.71 (C, thiazole), 124.48 (2 x CH, Ar), 126.76 (2 × CH, Ar), 129.09 (C, Ar), 140.85 (C, thiazole), 146.59 (C, Ar), 165.49 (C, thiazole), 170.71 (C=N), (CH_2-cyclopentyl signal missing due to overlap with DMSO-d_6). Anal. Calcd for $C_{15}H_{16}N_4O_2S$: C, 56.94; H, 5.10; N, 17.71. Found: C, 57.13; H, 4.98; N, 17.99.

8.4.3. 1-(4-(4-Cyanophenyl)thiazol-2-yl)-2-(2-methylcyclopentylidene)hydrazine (3)

E/*Z* ratio: 54/46. Yield 98%; mp 178–180 °C; IR cm^{-1} (KBr): 2231 (C≡N), 1619 (C=N); ^1H NMR ($CDCl_3$, 400 MHz) δ 1.20–1.22 (d, J = 6.7 Hz, 3H, CH_3), 1.22–1.23 (m, 1H, C_3H), 1.81–1.82 (m, 1H, cyclopentyl), 2.02–2.04 (m, 1H, cyclopentyl), 2.11–2.13 (m, 1H, cyclopentyl), 2.60–2.62 (m, 1H, cyclopentyl), 2.63–2.65 (m, 1H, cyclopentyl), 2.73–2.75 (m, 1H, cyclopentyl), 6.88 (s, 1H, C_5H-thiazole), 7.78–7.80 (d, J = 6.2 Hz, 2H, Ar), 7.85–7.87 (d, J = 6.2 Hz, 2H, Ar), 12.18 (br s, 1H, (*E*)-N*H*, D_2O exch.), 14.15 (br s, 1H, (*Z*)-N*H*, D_2O exch.); ^{13}C NMR (DMSO-d_6, 101 MHz) δ 17.36 (CH_3), 22.72 (CH_2, cyclopentyl), 29.29 (CH, cyclopentyl), 33.87 (CH_2, cyclopentyl), 107.76 (C, thiazole), 110.06 (C, Ar), 119.40 (C≡N), 126.61 (2 × CH, Ar), 133.12 (2 × CH, Ar), 138.74 (C, Ar), 147.94 (C, thiazole), 165.83 (C, thiazole), 170.61 (C=N), (CH_2-cyclopentyl signal missing due to overlap with DMSO-d_6). Anal. Calcd for $C_{16}H_{16}N_4S$: C, 64.84; H, 5.44; N, 18.90. Found: C, 65.01; H, 5.23; N, 19.19.

8.4.4. 1-(4-(2,4-Difluorophenyl)thiazol-2-yl)-2-(2-methylcyclopentylidene)hydrazine (4)

E/*Z* ratio: 56/44. Yield 99%; mp 160–163 °C; IR cm^{-1} (KBr): 3490 (N–H), 1618 (C=N), 1235 (Ar-F); ^1H NMR ($CDCl_3$, 600 MHz) δ 1.20–1.22 (d, J = 6.7 Hz, 3H, CH_3), 1.27–1.28 (m, 1H, cyclopentyl), 1.66–1.67 (m, 1H, cyclopentyl), 1.77–1.78 (m, 1H, cyclopentyl), 2.60–2.62 (m, 1H, cyclopentyl), 2.09–2.10 (m, 1H, cyclopentyl), 2.60–2.62 (m, 1H, cyclopentyl), 2.71–2.73 (m, cyclopentyl), 6.95 (s, 1H, C_5H-thiazole), 6.98–6.99 (ddd, J_{HF} = 11.4, 8.4 Hz, J_{HH} = 2.1 Hz,1H, Ar), 7.07–7.08 (dd, J_{HH} = 8.5 Hz, J_{HF} = 8.5 Hz, 1H, Ar), 7.85–7.87 (ddd, J_{HH} = 8.2 Hz, J_{HF} = 8.2, 6.2 Hz, 1H, Ar), 12.41 (br s, 1H, (*E*)-N*H*, D_2O exch.), 14.44 (br s, 1H, (*Z*)-N*H*, D_2O exch.). ^{13}C NMR ($CDCl_3$, 150 MHz) δ 16.71 (CH_3), 22.73 (CH_2, cyclopentyl), 30.61 (CH, cyclopentyl), 33.97 (CH_2, cyclopentyl), 40.18 (CH_2, cyclopentyl), 104.78 (d, J_{C-F} = 15.7 Hz, CH, thiazole), 105.45 (t, J_{C-F} = 26 Hz, CH, Ar), 112.69 (dd, J_{C-F} = 12 Hz, 3.6 Hz, C, Ar), 113.17 (dd, J_{C-F} = 22 Hz, 3.4 Hz, CH, Ar), 129.26 (d, J_{C-F} = 10 Hz, CH, Ar), 133.48 (C, thiazole), 160.30 (dd, J_{C-F} = 255 Hz, 12 Hz, CF, Ar), 163.58 (dd, J_{C-F} = 255 Hz, 12 Hz, CF, Ar), 169.08 (C, thiazole), 175.00 (C=N). Anal. Calcd for $C_{15}H_{15}F_2N_3S$: C, 58.62; H, 4.92; N, 13.67. Found: C, 58.89; H, 5.12; N, 13.49.

8.4.5. 1-(4-(4-Fluorophenyl)thiazol-2-yl)-2-(3-methylcyclopentylidene)hydrazine (5)

Yield 89%; mp 225–227 °C; IR cm^{-1} (KBr): 1615 (C=N), 1235 (Ar-F); ^1H NMR ($CDCl_3$, 600 MHz) δ 1.09–1.11 (d, J = 6.3 Hz, 3H, CH_3), 1.38–1.40 (m, 1H, cyclopentyl), 1.50–1.51 (m, 1H, cyclopentyl), 2.01–2.03 (m, 1H, cyclopentyl), 2.17–2.19 (m, 1H, cyclopentyl), 2.23–2.25 (m, 1H, cyclopentyl), 2.57–2.58 (m, 1H, cyclopentyl), 2.71–2.73 (m, 1H, cyclopentyl), 6.63 (s, 1H, C_5H-thiazole), 7.18–7.20 (dd, J_{HF} = 8.5 Hz, J_{HH} = 8.5 Hz, 2H, Ar), 7.70–7.72 (dd, J_{HH} = 8.6 Hz, J_{HF} = 5.0 Hz, 2H, Ar), 12.23 (br s, 1H, N*H*, D_2O exch.). ^{13}C NMR ($CDCl_3$, 150 MHz) δ 19.56, 19.96 (CH_3, cyclopentyl), 30.41, 32.74, 33.07, 33.08, 33.56, 33.75, 38.34, 41.56 (CH, CH_2, cyclopentyl), 100.10, 100.14 (CH, thiazole), 116.95 (d, J_{C-F} = 22 Hz, CH, Ar), 123.98 (d, J_{C-F} = 3.5 Hz, C, Ar), 127.84 (d, J_{C-F} = 8.7 Hz, CH, Ar), 139.55, 139.60 (C, thiazole),163.84 (d, J_{C-F} = 252 Hz, CF, Ar), 169.41, 169.47 (C, thiazole), 172.14, 172.24 (C=N). Anal. Calcd for $C_{15}H_{16}FN_3S$: C, 62.26; H, 5.57; N, 14.52. Found: C, 61.99; H, 5.41; N, 14.29.

8.4.6. 1-(3-Methylcyclopentylidene)-2-(4-(4-nitrophenyl)thiazol-2-yl) hydrazine (6)

Yield 96%; mp 176–177 °C; IR cm^{-1} (KBr): 1620 (C=N), 1517 and 1346 (NO_2); ^1H NMR (DMSO-d_6) δ 1.03 (s, 3H, CH_3), 1.70–1.72 (m, 1H, cyclopentyl), 1.89–1.91 (m, 1H, cyclopentyl), 1.93–1.96 (m, 1H, cyclopentyl), 2.02–2.04 (m, 1H, cyclopentyl), 2.35–2.37 (m, 1H, cyclopentyl), 2.47–2.49 (m, 1H, cyclopentyl), 2.75–2.77 (m, cyclopentyl), 7.62 (s, 1H, C_5H-thiazole), 8.08–8.10 (d, J = 8.9 Hz, 2H, Ar), 8.25–8.27 (d, J = 8.9 Hz, 1H, Ar), 10.74 (br s, 1H, N*H*, D_2O exch.); ^{13}C NMR (DMSO-d_6, 101 MHz) δ 19.83 (CH_3), 20.34 (CH_2, cyclopentyl), 29.21 (CH, cyclopentyl), 32.93 (CH_2, cyclopentyl), 41.36 (CH_2, cyclopentyl), 108.66 (C, thiazole), 124.51 (2 × CH, Ar), 126.85 (2 × CH, Ar), 140.65 (C, Ar), 146.61 (C, thiazole), 147.76 (C, Ar), 163.27 (C, thiazole), 170.30 (C=N). Anal. Calcd for $C_{15}H_{16}N_4O_2S$: C, 56.94; H, 5.10; N, 17.71. Found: C, 57.20; H, 4.90; N, 18.01.

8.4.7. 1-(4-(4-Cyanophenyl)thiazol-2-yl)-2-(3-methylcyclopentylidene)hydrazine (7)

E/*Z* ratio: 54/46. Yield 98%; mp 180–182 °C; IR cm^{-1} (KBr): 2229 (C≡N), 1620 (C=N); ^1H NMR ($CDCl_3$, 400 MHz) δ 1.09–1.11 (br s, 3H, CH_3), 1.54–1.55 (m, 1H, cyclopentyl), 1.56–1.58 (m, 1H, cyclopentyl), 1.59–1.61 (m, 1H, cyclopentyl), 2.36–2.38 (m, 1H, cyclopentyl), 2.52–2.54 (m, 1H, cyclopentyl), 2.66–2.68 (m, 1H, cyclopentyl), 2.83–2.85 (m, 1H, cyclopentyl), 6.87 (s, 1H, C_5H-thiazole), 7.77–7.78 (d, J_o = 8.2 Hz, 2H, Ar), 7.84–7.87 (d, J_o = 8.2 Hz, 2H, Ar), 12.15 (br s, 1H, (*E*)-N*H*, D_2O exch.), 14.21 (br s, 1H, (*Z*)-N*H*, D_2O exch.); ^{13}C NMR (DMSO-d_6, 101 MHz) δ 19.82 (CH_3), 20.32 (CH_2, cyclopentyl), 29.32 (CH, cyclopentyl), 32.93 (CH_2, cyclopentyl), 41.37 (CH_2, cyclopentyl), 107.74 (C, thiazole), 110.20 (C, Ar), 119.35 (C≡N), 126.70 (2 × CH, Ar), 133.12 (2 × CH, Ar), 138.32 (C, Ar), 147.32 (C, thiazole), 163.94 (C, thiazole), 170.14 (C=N). Anal. Calcd for $C_{16}H_{16}N_4S$: C, 64.84; H, 5.44; N, 18.90. Found: C, 65.04; H, 5.29; N, 19.10.

8.4.8. 1-(4-(2,4-Difluorophenyl)thiazol-2-yl)-2-(3-methylcyclopentylidene)hydrazine (8)

E/*Z* ratio: 53/47. Yield 88%; mp 131–134 °C; IR cm^{-1} (KBr): 3498 (N–H), 1598 (C=N), 1238 (Ar-F); ^1H NMR ($CDCl_3$, 600 MHz) δ 1.11–1.12 (br s, 3H, CH_3), 1.42–1.45 (m, 1H, cyclopentyl), 1.47–1.51 (m, 1H, cyclopentyl), 2.43–2.46 (m, 1H, cyclopentyl), 2.61–2.64 (m, 1H,

cyclopentyl), 2.67–2.69 (m, 1H, cyclopentyl), 2.78–2.80 (m, 1H, cyclopentyl), 2.84–2.86 (m, 1H, cyclopentyl), 6.91 (s, 1H, C_5H-thiazole), 6.94–6.99 (m, 1H, Ar) 7.07–7.11 (m, 1H, Ar), 7.88–7.91 (m, 1H, Ar), 12.36 (br s, 1H, (*E*)-N*H*, D_2O exch.), 14.40 (br s, 1H, (*Z*)-N*H*, D_2O exch.). ^{13}C NMR (DMSO-d_6, 150 MHz) δ 19.77, 20.30 (CH_3, cyclopentyl), 29.04, 32.73, 32.81, 32.86, 33.00, 33.21, 37.44, 41.30 (CH, CH_2 cyclopentyl), 104.89 (t, J_{C-F} = 26 Hz, CH, Ar), 107.68 (d, J_{C-F} = 13 Hz, CH, thiazole), 112.16 (dd, J_{C-F} = 21 Hz, 3.6 Hz, CH, Ar), 119.21 (C, Ar), 130.77 (dd, J_{C-F} = 10 Hz, 4.5 Hz, CH, Ar), 142.66 (C, thiazole), 159.89 (dd, J_{C-F} = 252 Hz, 12 Hz, CF, Ar), 161.61 (dd, J_{C-F} = 247 Hz, 12 Hz, CF, Ar), 162.79 (C, thiazole), 169.40 (C=N). Anal. Calcd for $C_{15}H_{15}F_2N_3S$: C, 58.62; H, 4.92; N, 13.67. Found: C, 58.96; H, 5.19; N, 13.89.

8.4.9. (*R*)-1-(4-(2,4-Difluorophenyl)thiazol-2-yl)-2-(3-methylcyclopentylidene)hydrazine ((*R*)-8)

E/*Z* ratio: 57/43. Yield 97%; mp 134–135 °C; IR cm^{-1} (KBr): 3474 (N–H), 1597 (C=N), 1234 (Ar-F); ^1H NMR ($CDCl_3$, 400 MHz) δ 1.10–1.16 (m, 3H, CH_3), 1.45–1.47 (m, 1H, cyclopentyl), 1.55–1.57 (m, 1H, cyclopentyl), 2.12–2.13 (m, 1H, cyclopentyl), 2.15–2.17 (m, 1H, cyclopentyl), 2.22–2.24 (m, 1H, cyclopentyl), 2.52–2.53 (m, 1H, cyclopentyl), 2.67–2.68 (m, 1H, cyclopentyl), 6.94 (s, 1H, C_5H-thiazole), 7.00–7.03 (m, 1H, Ar), 7.06–7.08 (m, 1H, Ar), 7.85–7.87 (m, 1H, Ar), 12.37 (br s, 1H, (*E*)-N*H*, D_2O exch.), 14.25 (br s, 1H, (*Z*)-N*H*, D_2O exch.). Anal. Calcd for $C_{15}H_{15}F_2N_3S$: C, 58.62; H, 4.92; N, 13.67. Found: C, 58.34; H, 4.79; N, 13.89.

8.4.10. (*Z*)-(*R*)-1-(4-(2,4-Difluorophenyl)thiazol-2-yl)-2-(3-methylcyclopentylidene)hydrazine ((*Z*)-(*R*)-8)

^1H NMR (DMSO-d_6, 600.13 MHz) δ 1.04 (d, J = 6.6 Hz, 3H, CH_3), 1.29 (m, 1H, CH_2 (c)), 1.88 (m, 2H, CH_2 (c), CH_2 (a)), 2.15 (m, 1H, CH (b)), 2.39 (dddd, J = 17.0; 9.8; 7.8; 2.0 Hz, 1H, CH_2 (d)), 2.43 (ddd, J = 17.0; 7.8; 3.8 Hz, 1H, CH_2 (d)), 2.66 (dd, J = 18.2; 7.8 Hz, 1H, CH_2 (a)), 7.11 (d, J_{H-F} = 2.5, 1H, C_5H-thiazole), 7.16 (ddd, J_{H-H} = 8.8; 2.7 Hz, J_{H-F} = 8.8 Hz, 1H, C_3H, Ar), 7.32 (ddd, J_{H-H} = 2.7 Hz, J_{H-F} = 11.7; 9.3 Hz, 1H, C_5H, Ar), 8.03 (ddd, J_{H-H} = 8.8 Hz, J_{H-F} = 8.8; 6.9 Hz 1H, C_2H, Ar), 10.58 (br s, 1H, (*Z*)-N*H*, D_2O exch.). ^{13}C NMR (DMSO-d_6, 150 MHz) δ 20.60 (CH_3, cyclopentyl), 33.00, 33.10, 33.40, 37.50 (CH, CH_2 cyclopentyl), 105.00 (t, J_{C-F} = 26 Hz, CH, Ar), 107.80 (d, J_{C-F} = 13 Hz, CH, thiazole), 112.30 (dd, J_{C-F} = 21 Hz, 3.6 Hz, CH, Ar), 119.21 (C, Ar), 130.80 (dd, J_{C-F} = 10 Hz, 4.5 Hz, CH, Ar), 159.89 (dd, J_{C-F} = 252 Hz, 12 Hz, CF, Ar), 161.61 (dd, J_{C-F} = 247 Hz, 12 Hz, CF, Ar), 162.79 (C, thiazole), 169.40 (C=N).

8.4.11. (*E*)-(*R*)-1-(4-(2,4-Difluorophenyl)thiazol-2-yl)-2-(3-methylcyclopentylidene)hydrazine ((*E*)-(*R*)-8)

^1H NMR (DMSO-d_6; 600.13 MHz) δ 1.02 (d, J = 6.6 Hz, 3H, CH_3), 1.37 (m, 1H, CH_2 (c)), 1.95 (m, 1H, CH_2 (c)), 2.01 (m, 1H, CH_2 (a)), 2.06 (m, 1H, CH (b)), 2.30 (m, 1H, CH_2 (d)), 2.50 (m, 1H, CH_2 (d), CH_2 (a)), 7.11 (d, J_{H-F} = 2.5, 1H, C_5H-thiazole), 7.16 (ddd, J_{H-H} = 8.8; 2.7 Hz, J_{H-F} = 8.8 Hz, 1H, C_3H, Ar), 7.32 (ddd, J_{H-H} = 2.7 Hz, J_{H-F} = 11.7; 9.3 Hz, 1H, C_5H, Ar), 8.03 (ddd, J_{H-H} = 8.8 Hz, J_{H-F} = 8.8; 6.9 Hz 1H, C_2H, Ar), 10.60 (br s, 1H, (*E*)-N*H*, D_2O exch.).

8.4.12. HPLC diastereoseparation

Analytical HPLC analysis of rac-**8** was performed using commercially available 250 mm × 4.6 mm I.D. Chiralpak AD column (Chiral Technologies Europe, Illkirch, France). HPLC grade solvents were purchased from Aldrich (St. Louis, Missouri USA). Semi-preparative HPLC diastereoseparation of (*R*)-**8** was performed using commercially available 250 mm × 10 mm I.D. Chiralpak AD column. The analytical HPLC apparatus consisted of a Perkin–Elmer (Norwalk, CT, USA) 200 LC pump equipped with a Rheodyne (Cotati, CA, USA) injector, a 20 mL sample loop, an HPLC Dionex CC-100 oven (Sunnyvale, CA, USA) and a Jasco Model CD 2095 Plus UV/CD detector (Jasco, Tokyo, Japan). Semi-preparative separations were carried out with a Perkin–Elmer (Norwalk, CT, USA) 200 LC pump equipped with a Rheodyne (Cotati, CA, USA) injector, a 1 mL sample loop, a Perkin-Elmer LC 101 oven, and a Waters 484 detector (Waters Corporation, Milford, MA, USA). The signal was acquired and processed by Clarity software (DataApex, Prague, The Czech Republic).

8.4.13. Polarimetry

Specific rotations of the distereomers of (*R*)-**8** were measured at 589 nm by a Perkin-Elmer polarimeter model 241 equipped with a Na/Hg lamp. The volume of the cell was 1 mL and the optical path was 10 cm. The system was set to 20 °C.

8.4.14. *E*/*Z* Assignment of geometric isomers of compound (*R*)-8

Sample was dissolved in DMSO-d_6. The NMR spectra were recorded at 27 °C on a Bruker AVANCE600 NMR spectrometer operating at the proton frequency of 600.13 MHz and equipped with a Bruker multinuclear z-gradient inverse probehead. Chemical shifts (δ-scale) of proton spectra are reported with respect to the solvent residual signal at 2.50 ppm. ^1H–^1H COSY experiment was acquired using 2048 data points in f2, 256 increments in f1, spectral width 6.6 kHz in both dimensions, 3 s recycle delay. ^1H–^1H NOESY experiment was recorded in the phase sensitive mode (TPPI) with a mixing time of 0.8 s and by using the following parameters: a spectral width of 6.6 kHz in both dimensions, 1024 data points in f2, 512 increments in f1, a recycle delay of 3 s, 16 dummy scans and 16 scans; the data were processed with an squared sine window function and a 1024 × 1024 data matrix size.

8.4.15. Determination of hMAO isoform activity

The effects of the test compounds on the enzymatic activity of hMAO isoform were evaluated by a fluorimetric method following the experimental protocol previously described by us.[19] Sodium phosphate buffer (0.1 mL, 0.05 M, pH 7.4) containing different concentrations of the test drugs (new compounds or reference inhibitors) and adequate amounts of recombinant hMAO-A or hMAO-B required and adjusted to obtain the same reaction velocity in our experimental conditions, that is, to oxidize (in the control group) 165 pmol of *p*-tyramine/min, were incubated for 15 min at 37 °C in a flat-black-bottom 96-well microtest™ plate (BD Biosciences, Franklin Lakes, NJ, USA) placed in a dark fluorimetric chamber. After this incubation period, the reaction was started by adding (final concentrations) 200 μM Amplex® Red reagent, 1 U/mL horseradish peroxidase and 1 mM *p*-tyramine. The production of H_2O_2 and, consequently, of resorufin was quantified at 37 °C in a multidetection microplate fluorescence reader (Fluostar Optima, BMG Labtech GmbH, Offenburg, Germany) based on the fluorescence generated (excitation, 545 nm, emission, 590 nm) over a 15 min period, in which the fluorescence increased linearly.

Control experiments were carried out simultaneously by replacing the test drugs with appropriate dilutions of the vehicles. In addition, the potential ability of the above test drugs to modify the fluorescence generated in the reaction mixture due to non-enzymatic inhibition was determined by adding these drugs to solutions containing only the Amplex® Red reagent in a sodium phosphate buffer. To determine the kinetic parameters of hMAO-A and hMAO-B (K_m and V_{max}), the corresponding enzymatic activity of both isoforms was evaluated in presence of a wide range of *p*-tyramine concentrations. The specific fluorescence emission was calculated after subtraction of the background activity, which was determined from vials containing all components except the hMAO isoforms.

The drugs, vehicle and chemicals used in the experiments were the new compounds, moclobemide (F. Hoffmann-La Roche Ltd, Basel, Switzerland), dimethyl sulfoxide, *R*-(−)-deprenyl hydrochloride, iproniazid phosphate and isatin (Sigma–Aldrich, Spain),

resorufin sodium salt, clorgyline hydrochloride, *p*-tyramine hydrochloride, sodium phosphate and horseradish peroxidase (supplied in the Amplex® Red MAO assay kit from Molecular Probes). Unless otherwise specified, results shown in the text and tables are expressed as mean ± standard error of the mean (S.E.M.) from *n* experiments. Significant differences between two means ($P < 0.05$ or $P < 0.01$) were determined by one-way analysis of variance (ANOVA) followed by the Dunnett's *post-hoc* test. Graph Pad Prism Software (GraphPad Software, San Diego, California, USA) was used to perform statistical analyses and to calculate IC_{50} values and kinetic parameters.

8.4.16. Molecular modeling

The Scrodinger Suite 2013-1 was used for all molecular modeling tasks.[20] The hMAO-A and hMAO-B enzyme models were obtained from the Protein Data Bank[21] (PDB) crystallographic structures 2Z5X[22] and 2V5Z,[23] respectively. The selected PDB entries represented the best crystallographic resolution structures of human MAO isoforms in non-covalent complexes with known inhibitors available. In both enzyme models the original co-crystallized ligands and water molecules were removed, FAD double bonds were fixed and hydrogen atoms were added. The conformational properties of both *E* and *Z* isomers of (*R*)-**8** were explored by means of 2000 steps of Monte Carlo (MC) search applied to the ligands rotatable bonds. The energy evaluation of the MC structures was carried out with the OPLS-AA[24] force field and solvent effects were taken into using the implicit solvation model GB/SA water.[25] Both (*E*)-(*R*)-**8** and (*Z*)-(*R*)-**8** highlighted 6 unique conformations within 12 kcal/mol above the global minimum energy ones. The energy difference between the most energy stable conformers of *E* and *Z* isomers was equal to 0.89 kcal/mol in favor of the *E* form. Boltzmann analysis, computed at 300 K, was applied to MC ensembles. The global minimum energy structures, in both cases reporting a population larger than 86%, were submitted to Glide[26] docking simulations with respect to hMAO-A and -B theoretical models. A regular box, of about 110,000 Å^3, centered onto the FAD N5 atom, was considered as the enzyme active site for both hMAO-A and -B. Induced fit phenomena were taken into account using the ligand flexible algorithm. The binding affinity was estimated by means of the Glide XP scoring function (GScoreXP). The top ranked complexes were considered for the binding modes graphical analysis. PyMol software[27] was used for depicting molecular modeling figures and for calculating the enzyme bind clefts shape.

Acknowledgments

This work was supported by 'FILAS' - 'Italy' (research project n° ASR2, Regione Lazio, Italy).

Supplementary data

Supplementary data associated with this article can be found, in the online version, at http://dx.doi.org/10.1016/j.bmc.2014.03.042.

References and notes

1. (a) Murphy, D. L. *Biochem. Pharmacol.* **1889**, *1978*, 27; (b) Bach, A. W.; Lan, N. C.; Johnson, D. L.; Abell, C. W.; Bembenek, M. E.; Kwan, S.-W.; Seeburg, P. H.; Shih, J. C. *PNAS* **1988**, *85*, 4934; (c) Westlund, K. N.; Denney, R. M.; Rose, R. M.; Abell, C. W. *Neuroscience* **1988**, *25*, 439; (d) Edmondson, D. E.; Mattevi, A.; Binda, C.; Li, M.; Hubálek, F. *Curr. Med. Chem.* **1983**, *2004*, 11; (e) Edmondson, D. E.; Binda, C.; Wang, J.; Upadhayay, A. K.; Mattevi, A. *Biochemistry* **2009**, *48*, 4220.
2. Shih, J. C.; Chen, K.; Ridd, M. J. *Annu. Rev. Neurosci.* **1999**, *22*, 197.
3. (a) Shih, J. C.; Chen, K. *Curr. Med. Chem.* **2004**, *11*, 1995; (b) Sayre, L. M.; Perry, G.; Smith, M. A. *Chem. Res. Toxicol.* **2008**, *21*, 172.
4. Blandini, F. *CNS Drug Rev.* **2005**, *11*, 183.
5. (a) Riederer, P.; Lachenmayer, L.; Laux, G. *Curr. Med. Chem.* **2004**, *11*, 2033; (b) Youdim, M. B. H.; Edmondson, D. E.; Tipton, K. F. *Nat. Rev.* **2006**, *7*, 295; (c) Bortolato, M.; Chen, K.; Shih, J. C. *Adv. Drug Deliv. Rev.* **2008**, *60*, 1527.
6. (a) Bolasco, A.; Fioravanti, R.; Carradori, S. *Expert Opin. Ther. Patents* **2005**, *15*, 1763; (b) Bolasco, A.; Carradori, S.; Fioravanti, R. *Expert Opin. Ther. Patents* **2010**, *20*, 909; (c) Carradori, S.; Secci, D.; Bolasco, A.; Chimenti, P.; D'Ascenzio, M. *Expert Opin. Ther. Patents* **2012**, *22*, 759; (d) Carradori, S.; D'Ascenzio, M.; Chimenti, P.; Secci, D.; Bolasco, A. *Mol. Div.* **2014**, *18*, 219.
7. Chimenti, P.; Petzer, A.; Carradori, S.; D'Ascenzio, M.; Silvestri, R.; Alcaro, S.; Ortuso, F.; Petzer, J. P.; Secci, D. *Eur. J. Med. Chem.* **2013**, *66*, 221.
8. Chimenti, F.; Maccioni, E.; Secci, D.; Bolasco, A.; Chimenti, P.; Granese, A.; Carradori, S.; Alcaro, S.; Ortuso, F.; Yáñez, M.; Orallo, F.; Cirilli, R.; Ferretti, R.; La Torre, F. *J. Med. Chem.* **2008**, *51*, 4874.
9. Chimenti, F.; Carradori, S.; Secci, D.; Bolasco, A.; Chimenti, P.; Granese, A.; Bizzarri, B. *J. Heterocycl. Chem.* **2009**, *46*, 575.
10. Chimenti, F.; Secci, D.; Bolasco, A.; Chimenti, P.; Granese, A.; Carradori, S.; Maccioni, E.; Cardia, M. C.; Yáñez, M.; Orallo, F.; Alcaro, S.; Ortuso, F.; Cirilli, R.; Ferretti, R.; Distinto, S.; Kirchmair, J.; Langer, T. *Bioorg. Med. Chem.* **2010**, *18*, 5063.
11. Chimenti, F.; Secci, D.; Bolasco, A.; Chimenti, P.; Granese, A.; Carradori, S.; Yáñez, M.; Orallo, F.; Ortuso, F.; Alcaro, S. *Bioorg. Med. Chem.* **2010**, *18*, 5715.
12. Chimenti, F.; Secci, D.; Bolasco, A.; Chimenti, P.; Granese, A.; Carradori, S.; D'Ascenzio, M.; Yáñez, M.; Orallo, F. *Med. Chem. Commun.* **2010**, *1*, 61.
13. Chimenti, F.; Secci, D.; Bolasco, A.; Chimenti, P.; Granese, A.; Carradori, S.; Yáñez, M.; Orallo, F.; Sanna, M. L.; Gallinella, B.; Cirilli, R. *J. Med. Chem.* **2010**, *53*, 6516.
14. Secci, D.; Bolasco, A.; Carradori, S.; D'Ascenzio, M.; Nescatelli, R.; Yáñez, M. *Eur. J. Med. Chem.* **2012**, *58*, 405.
15. Carradori, S.; D'Ascenzio, M.; De Monte, C.; Secci, D.; Yáñez, M. *Arch. Pharm. Life Sci.* **2013**, *346*, 17.
16. Benassi, R.; Benedetti, A.; Taddei, F.; Cappelletti, R.; Nardi, D.; Tajana, A. *Org. Magn. Reson.* **1982**, *20*, 26.
17. Cirilli, R.; Ferretti, R.; La Torre, F.; Secci, D.; Bolasco, A.; Carradori, S.; Pierini, M. *J. Chromatogr. A* **2007**, *1172*, 160.
18. Carradori, S.; Cirilli, R.; Dei Cicchi, S.; Ferretti, R.; Menta, S.; Pierini, M.; Secci, D. *J. Chromatogr. A* **2012**, *1269*, 168.
19. Yáñez, M.; Fraiz, N.; Cano, E.; Orallo, F. *Biochem. Biophys. Res. Commun.* **2006**, *344*, 688.
20. Schrödinger, LLC; New York, NY, 2013. http://www.schrodinger.com.
21. Berman, H. M.; Westbrook, J.; Feng, Z.; Gilliland, G.; Bhat, T. N.; Weissig, H.; Shindyalov, I. N.; Bourne, P. E. *Nucleic Acids Res.* **2000**, *28*, 235.
22. Son, S. Y.; Ma, J.; Kondou, Y.; Yoshimura, M.; Yamashita, E.; Tsukihara, T. *Proc. Natl. Acad. Sci. U.S.A.* **2008**, *105*, 5739.
23. Binda, C.; Wang, J.; Pisani, L.; Caccia, C.; Carotti, A.; Salvati, P.; Edmondson, D. E.; Mattevi, A. *J. Med. Chem.* **2007**, *50*, 5848.
24. Kaminski, G. A.; Friesner, R. A.; Tirado-Rives, J.; Jorgensen, W. J. *J. Phys. Chem. B* **2001**, *105*, 6474.
25. Hasel, W.; Hendrickson, T. F.; Still, W. C. *Tetrahedron Comput. Methodol.* **1988**, *1*, 103.
26. (a) Friesner, R. A.; Murphy, R. B.; Repasky, M. P.; Frye, L. L.; Greenwood, J. R.; Halgren, T. A.; Sanschagrin, P. C.; Mainz, D. T. *J. Med. Chem.* **2006**, *49*, 6177; (b) Halgren, T. A.; Murphy, R. B.; Friesner, R. A.; Beard, H. S.; Frye, L. L.; Pollard, W. T.; Banks, J. L. *J. Med. Chem.* **2004**, *47*, 1750; (c) Friesner, R. A.; Banks, J. L.; Murphy, R. B.; Halgren, T. A.; Klicic, J. J.; Mainz, D. T.; Repasky, M. P.; Knoll, E. H.; Shaw, D. E.; Shelley, M.; Perry, J. K.; Francis, P.; Shenkin, P. S. *J. Med. Chem.* **2004**, *47*, 1739.
27. The PyMOL Molecular Graphics System, Version 1.3 Schrödinger, LLC. http://www.schrodinger.com.